



Investigation of the backbone dynamics of the IgG-binding domain of streptococcal protein G by heteronuclear two-dimensional ^1H - ^{15}N nuclear magnetic resonance spectroscopy

JOSEPH J. BARCHI, JR.,¹ BRUCE GRASBERGER,^{2,3} ANGELA M. GRONENBORN,²
AND G. MARIUS CLORE²

¹Laboratory of Medicinal Chemistry, Developmental Therapeutics Program, Building 37,
National Cancer Institute, Bethesda, Maryland 20892

²Laboratory of Chemical Physics, Building 5, National Institute of Diabetes, Digestive and Kidney Diseases,
National Institutes of Health, Bethesda, Maryland 20892

(RECEIVED October 7, 1993; ACCEPTED November 5, 1993)

Abstract

The backbone dynamics of the immunoglobulin-binding domain (B1) of streptococcal protein G, uniformly labeled with ^{15}N , have been investigated by two-dimensional inverse detected heteronuclear ^1H - ^{15}N NMR spectroscopy at 500 and 600 MHz. ^{15}N T_1 , T_2 , and nuclear Overhauser enhancement data were obtained for all 55 backbone NH vectors of the B1 domain at both field strengths. The overall correlation time obtained from an analysis of the T_1/T_2 ratios was 3.3 ns at 26 °C. Overall, the B1 domain is a relatively rigid protein, consistent with the fact that over 95% of the residues participate in secondary structure, comprising a four-stranded sheet arranged in a $-1, +3x, -1$ topology, on top of which lies a single helix. Residues in the turns and loops connecting the elements of secondary structure tend to exhibit a higher degree of mobility on the picosecond time scale, as manifested by lower values of the overall order parameter. A number of residues at the ends of the secondary structure elements display two distinct internal motions that are faster than the overall rotational correlation time: one is fast (<20 ps) and lies in the extreme narrowing limit, whereas the other is one to two orders of magnitude slower (1–3 ns) and lies outside the extreme narrowing limit. The slower motion can be explained by large-amplitude (20 – 40°) jumps in the N-H vectors between states with well-defined orientations that are stabilized by hydrogen bonds. In addition, residues in the helix and in the outer β -strands (particularly β -strand 2) display a small degree of chemical exchange line broadening, possibly due to a minor rotational motion of the helix relative to the sheet that curls around it.

Keywords: heteronuclear relaxation; IgG-binding domain of protein G; protein dynamics

Streptococcal protein G contains repeats of two or more immunoglobulin-binding domains, each comprising 55 or 56 residues (Boyle, 1990; Fahnestock et al., 1990). These domains are unusual in that they exhibit extreme stability to both heat and urea denaturation, despite the absence of any disulfide bridges (Gronenborn et al., 1991; Gronenborn & Clore, 1993a). In a series of recent papers, we have solved the three-dimensional solution structure of the B1 domain of protein G at very high resolution by NMR (Gronenborn et al., 1991; Clore et al., 1993), determined the location of tightly bound water molecules within

the solution structure (Clore & Gronenborn, 1992), and identified the contact site on the B1 domain complexed with IgG_{FC} (the C-terminal fragment of the heavy chain of immunoglobulin G) (Gronenborn & Clore, 1993b). Subsequent to the NMR structure determination, the crystal structure of the related B2 domain was solved at 1.67 Å resolution (Achari et al., 1992). The structural studies have revealed a highly compact globular protein with a tightly packed hydrophobic core in which 95% of the residues participate in regular secondary structure. The domain is made up of a four-stranded β -sheet consisting of two antiparallel β -hairpins connected by an α -helix, arranged in an unusual $-1, +3x, -1$ topology (see Kinemage 1).

The internal dynamics of proteins play an important role in the interplay between protein structure and function (Ringe & Petsko, 1985). In this paper we have therefore extended our previous structural studies on the B1 domain of protein G to an

Reprint requests to: Angela M. Gronenborn or G. Marius Clore, Laboratory of Chemical Physics, Building 5, National Institute of Diabetes, Digestive and Kidney Disease, National Institutes of Health, Bethesda, Maryland 20892.

³ Present address: Sterling Winthrop, Malvern, Pennsylvania 19426.

investigation of its backbone dynamics by means of ^{15}N relaxation measurements.

Results and discussion

The ^{15}N relaxation (i.e., ^{15}N T_1 , T_2 , and NOE) data at 26 °C were obtained at two spectrometer frequencies (500 and 600 MHz)

using pulse sequences described previously (Kay et al., 1989; Clore et al., 1990a) and appropriately modified to eliminate cross-correlation between dipolar and chemical shift anisotropy relaxation mechanisms (Boyd et al., 1990; Kay et al., 1992; Palmer et al., 1992). A ^1H - ^{15}N NOE correlation spectrum and some representative plots of ^{15}N T_1 and T_2 decays are shown in Figure 1, and a summary of the ^{15}N T_1 , T_2 , and NOE data, plot-

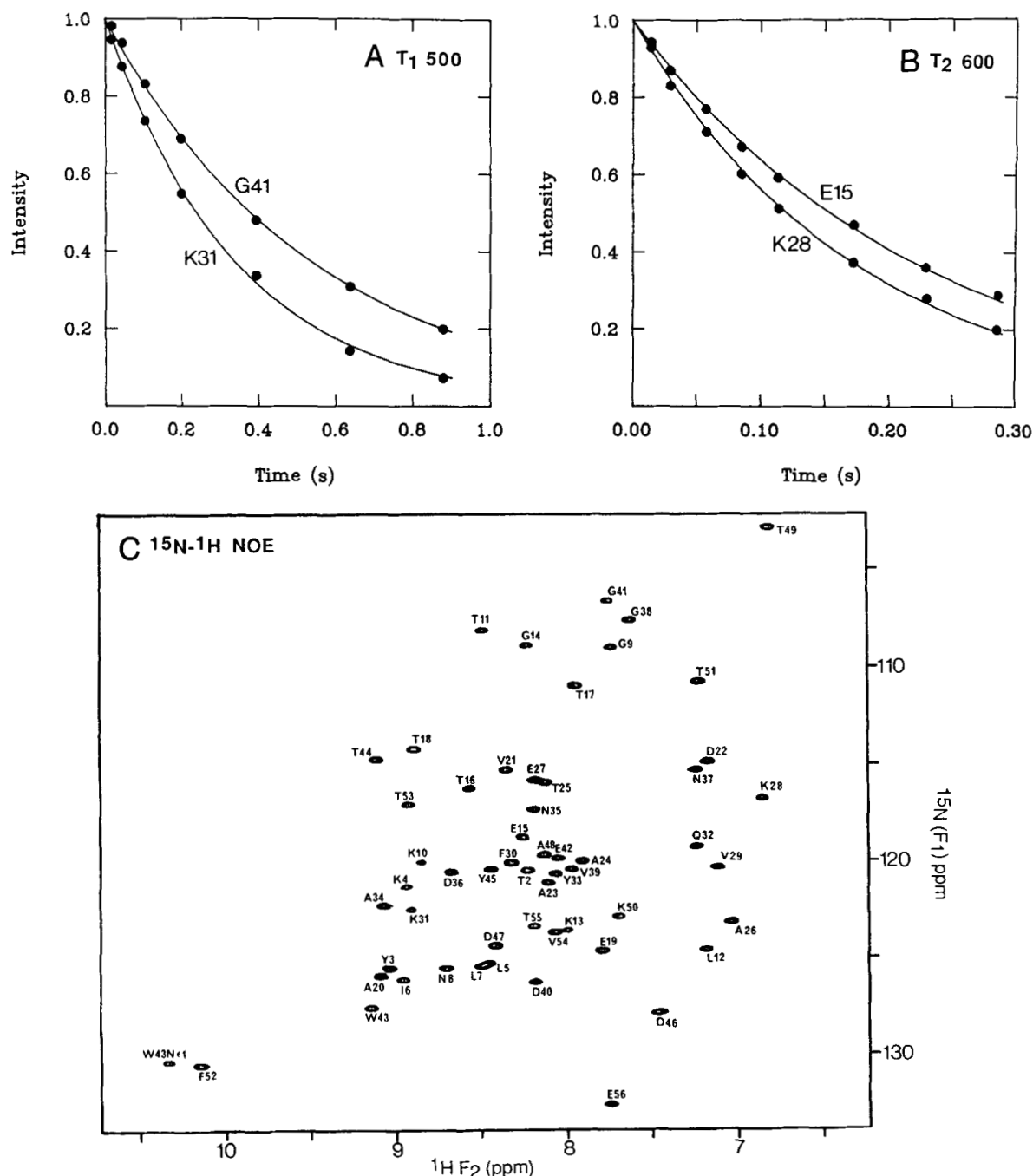


Fig. 1. A, B: Representative plots of cross-peak intensity versus delay time for the T_1 data at 500 MHz and the T_2 data at 600 MHz, respectively. C: ^{15}N - ^1H NOE correlation spectrum at 500 MHz for the IgG-binding domain of streptococcal protein G at 26 °C. In A and B, the solid lines represent single exponential best fits to the experimental data. Note that all the ^1H - ^{15}N NOEs in C are positive.

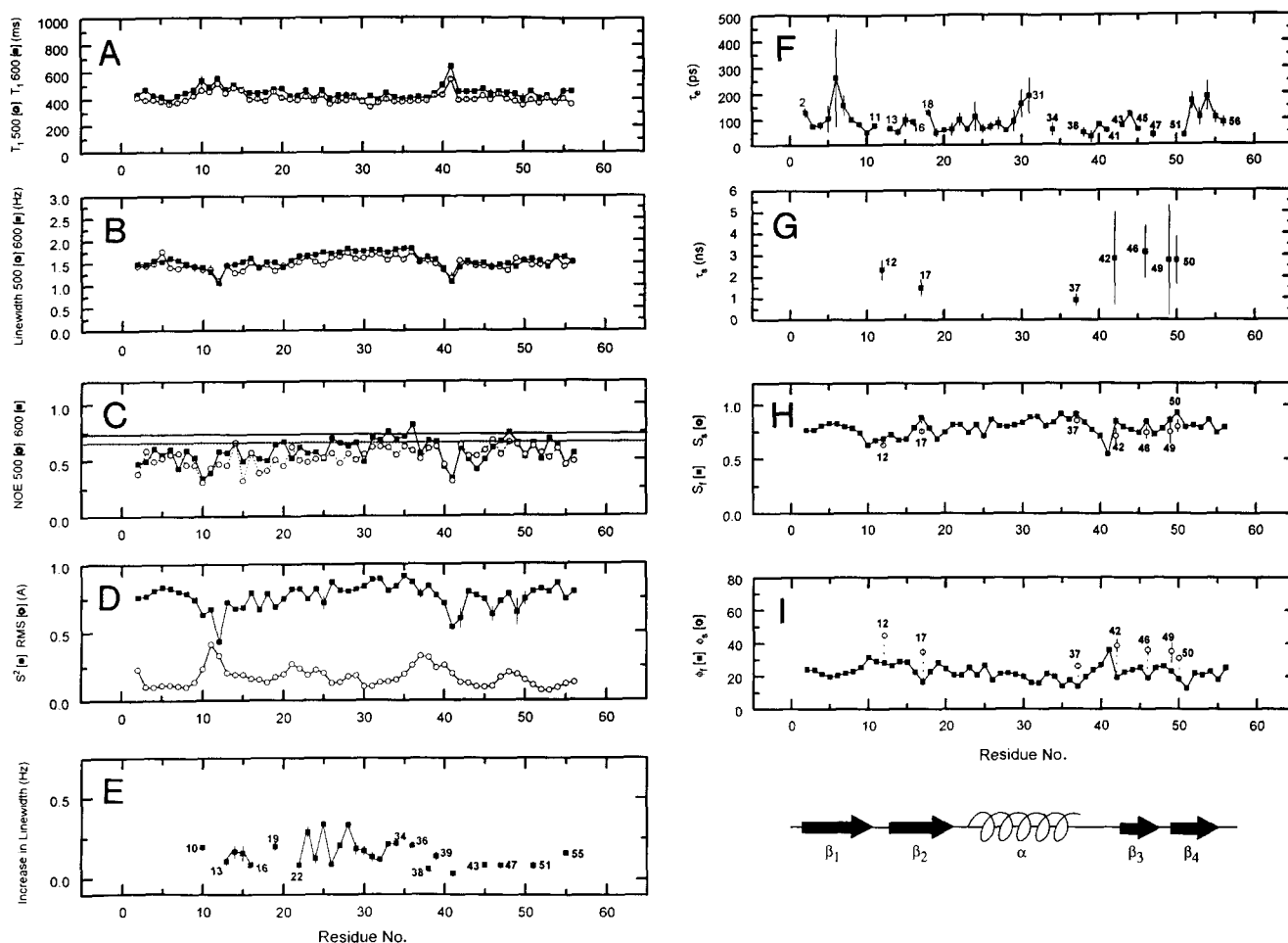


Fig. 2. Graphical representation as a function of residue number for the ^{15}N relaxation data and their analysis obtained at 500 and 600 MHz for the IgG-binding domain of protein G at 26 °C. The relaxation data at 500 and 600 MHz are shown as open circles and closed squares, respectively. **A:** ^{15}N T_1 . **B:** ^{15}N T_2 (displayed as linewidth = $1/\pi T_2$). **C:** ^{15}N - ^1H NOEs (the dotted and dashed horizontal lines indicate the maximum NOE at 500 and 600 MHz, respectively, for a rotational correlation time of 3.3 ns). **D:** Generalized overall order parameters S^2 (closed squares) calculated from the relaxation data, together with the atomic RMS distribution of the backbone amides (open circles) about the mean coordinates for the 60 calculated solution NMR structures of Gronenborn et al. (1991). **E:** Exchange linewidths for residues whose fit to the relaxation data required the use of Equations 1 and 2. **F:** Effective internal correlation time τ_e for residues whose relaxation data were fitted to the full Lipari and Szabo (1982) spectral density function given by Equation 4. **G:** Effective correlation time τ_s for the slower internal motion for residues whose relaxation data were fitted to the extended spectral density function of Clore et al. (1990b) given by Equation 5. **H:** Fast S_f^2 (closed squares) and slow S_s^2 (open circles) motion order parameters. (For residues that were fit to the conventional Lipari and Szabo [1982] spectral density function [either Equation 3 or 4] $S_f^2 = S^2$.) **I:** Values of the θ_f (closed squares) and ϕ_s (open circles) angles given by $S_f^2 = [0.5 \cos \theta_f (1 + \cos \theta_f)]^2$ and $S_s^2 = (1 + 3 \cos^2 \phi_s)/4$, respectively. θ_f is the semi-angle for free diffusion in a cone, and ϕ_s is the angle between the NH vectors in two states i and j for those residues whose relaxation data were fitted to the extended spectral density function given by Equation 5. The standard deviations of the experimental T_1 's and linewidths of the various calculated parameters are represented by vertical bars. The errors in the experimental ^1H - ^{15}N NOEs are on the order of ± 0.1 . The locations of the β -strands and helix are indicated below the figure.

ted as a function of residue number, is provided in Figure 2A–C. All backbone ^{15}N -NH cross peaks were clearly resolved at both 500 MHz and 600 MHz, so complete relaxation data could be obtained for the entire domain.

The overall rotational correlation time was obtained from the T_1/T_2 ratios (Kay et al., 1989; Clore et al., 1990a). The average T_1/T_2 ratio was 1.88 ± 0.12 and 2.16 ± 0.18 at 500 and 600 MHz, respectively. The overall rotational correlation time, τ_R , obtained by fitting all the data at 500 and 600 MHz simultaneously and excluding those residues with a ratio outside $\pm 1\text{SD}$ of the mean (Clore et al., 1990a), was 3.30 ± 0.02 ns. (Note that this

value differs minimally from that of 3.27 ± 0.04 ns obtained when the T_1/T_2 ratios for all residues are included in the fit.) The B1 domain is the smallest protein (56 residues) studied by ^{15}N relaxation measurements and hence displays the shortest τ_R . The value of τ_R for the B1 domain, however, is completely consistent with those of 4.1–4.2 ns obtained for eglin c (69 residues), calbindin D9k (75 residues), and ubiquitin (76 residues) (Peng & Wagner, 1992; Kördel et al., 1992; Schneider et al., 1992).

For each residue, the ^{15}N T_1 , T_2 , and NOE data at both spectrometer frequencies were fitted simultaneously to various

model-free spectral density functions in the presence and absence of an additional term ($\pi\Delta ex$) to account for the effect of chemical exchange line broadening on T_2 , as described by Clore et al. (1990a). This effect is given by

$$1/T_2(obs) = 1/T_2 + \pi\Delta ex. \quad (1)$$

Further, when exchange is fast on the chemical shift scale, the chemical exchange terms at the two spectrometer frequencies are related by

$$\pi\Delta ex(500) = \pi\Delta ex(600) \times 0.694, \quad (2)$$

where 0.694 is the ratio of the squares of the two spectrometer frequencies (i.e., $500^2/600^2$). Hence, only one chemical exchange term was optimized. The spectral density functions employed were the model-free spectral density function of Lipari and Szabo (1982) and the extended model-free spectral density function of Clore et al. (1990a, 1990b).

The data for 29 residues could be accounted for without introducing chemical exchange line broadening (i.e., $\pi\Delta ex = 0$). Of these 29 residues, only two (Asn 35 and Ala 48) could be accounted for by a simplified model-free spectral density function, $J(\omega_i)$, in which the internal correlation time, τ_e , is assumed to be less than 20 ps and hence does not contribute to $J(\omega_i)$:

$$J(\omega_i) = S^2\tau_R/(1 + \omega_i^2\tau_R^2), \quad (3)$$

where S^2 is the generalized overall order parameter (Lipari & Szabo, 1982). For Equation 3, the calculated NOE is at its maximum value for a given τ_R . For a rotational correlation time of 3.3 ns, the theoretical NOE maxima are 0.74 and 0.67 at spectrometer frequencies of 600 MHz and 500 MHz, respectively. Both Asn 35 and Ala 48 have NOE values close to the expected maximum values (Fig. 2C), as well as large values of S^2 . The data for 20 residues could be accounted for by the complete model-free spectral density function of Lipari and Szabo (1982):

$$J(\omega_i) = S^2\tau_R/(1 + \omega_i^2\tau_R^2) + (1 - S^2)\tau'_e/(1 + \omega_i^2\tau_e'^2), \quad (4)$$

where $\tau'_e = \tau_R\tau_e/(\tau_R + \tau_e)$. The values of τ_e ranged from 56 to 260 ps (Fig. 2F) and hence are still in the extreme narrowing limit. Finally, the data for seven residues necessitated the use of the extended model-free spectral density function (Clore et al., 1990a, 1990b):

$$J(\omega_i) = S^2\tau_R/(1 + \omega_i^2\tau_R^2) + S_f^2(1 - S_s^2)\tau'_s/(1 + \omega_i^2\tau_s'^2), \quad (5)$$

where S_f^2 and S_s^2 are the order parameters for the fast and slow motions; τ_s is the internal correlation time for the slow motions (with $\tau'_s = \tau_R\tau_s/(\tau_R + \tau_s)$); and the internal correlation time for the fast motions, τ_f , is assumed to be less than 20 ps so that terms containing τ_f are neglected. In this spectral density function, the slow motions lie outside the extreme narrowing limit (i.e., $250 \text{ ps} < \tau_s < \tau_R$). The values of τ_s ranged from 1.2 to 3.1 ns (Fig. 2G).

The data for the remaining 26 residues required the incorporation of a chemical exchange term for T_2 (i.e., Equation 1). Of these, 3 could be accounted for by Equation 3 and 23 by Equation 4.

The results of the analysis are displayed as a function of residue number in Figure 2. Figure 3A displays the variation of the generalized order parameter as a color gradient from red (highly mobile) to blue (low mobility) on the three-dimensional structure. Figure 3B shows the locations in the three-dimensional structure of the residues that fit the various spectral density functions (Equations 3, 4, and 5) with (Equations 1 and 2) or without chemical exchange.

The average value of the overall generalized order parameter S^2 for all 55 residues of the IgG-binding domain is 0.76 ± 0.09 , with S^2 ranging from 0.43 for Leu 12 to 0.92 for Asn 35. Only nine residues have values of S^2 outside $\pm 1SD$ of the average value, with six below (i.e., more mobile than average) and three above (less mobile than average). Excluding the 6 residues with S^2 values below 1SD of the mean value yields an average value of 0.79 ± 0.06 for the remaining 47 residues. This translates to an average semi-angle value of $23 \pm 4^\circ$ for free diffusion within a cone. Thus, overall the structure is fairly rigid on the picosecond time scale, as expected from the very high proportion ($\sim 95\%$) of residues involved in secondary structure (Gronenborn et al., 1991). In this regard, it should be noted that the N- and C-terminal residues are part of the β -sheet and consequently display average values of S^2 .

The regions that display the most significant mobility on the picosecond time scale (displayed in red, orange, and light green in Fig. 3A) are located in the turn connecting β -strands 1 and 2 (Lys 10 and Leu 12), in the loop connecting the helix with β -strand 3 (Gly 41 and Glu 42), and in the turn connecting β -strands 3 and 4 (Asp 46 and Thr 49) (Fig. 2D). In addition, it is interesting to note that β -strand 2, which has an average S^2 value of 0.72 ± 0.05 , is slightly more mobile than either the other three β -strands or the helix. This is clearly evident in Figure 3A, where β -strand 2 shows a preponderance of green residues (intermediate mobility), while the other strands and helix are mainly blue (low mobility). This may be due to steric considerations as the side chains of Lys 13 to Glu 19 vie for the most energetically favorable arrangement of alkyl groups within and on the periphery of the hydrophobic core.

Figure 2D also presents a comparison of the generalized order parameter S^2 with the average atomic RMS distribution (RMSD) of the 60 calculated NMR structures about their mean coordinate positions (taken from the high-resolution structure of Gronenborn et al., 1991) (see Kinemage 2). The degree of correspondence is similar to what has been observed previously (Redfield et al., 1992; Grasberger et al., 1993; Powers et al., 1993). That is, there is some evidence of an inverse correlation at a qualitative level. Thus, the largest RMSD and lowest S^2 values are located in the turn connecting β -strands 1 and 2. However, the correspondence is not exact. Thus, Thr 11 has the largest RMSD value, whereas Leu 12 has the lowest S^2 value. Similar observations can be made for the C-terminal end of the helix and the loop connecting the helix to β -strand 3, and for the turn connecting β -strands 3 and 4. As discussed by Powers et al. (1993), this simply reflects the facts that the relationship between S^2 and RMSD is indirect and that the RMSD depends purely on the number and distribution of the interproton distance restraints. These interproton distance restraints are related not only to dynamics on

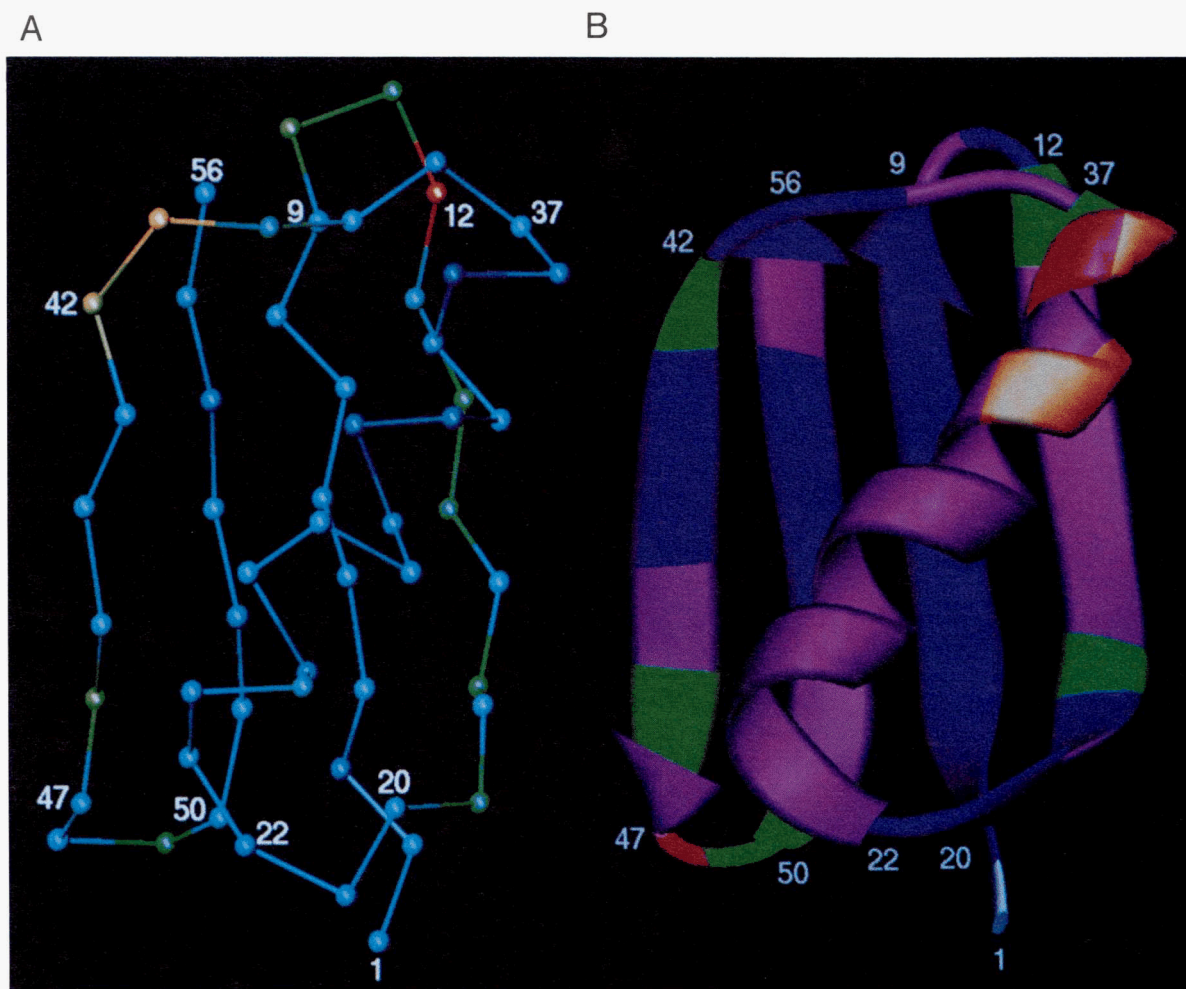


Fig. 3. **A:** C α trace of the IgG-binding domain of protein G color-coded for the generalized order parameter S^2 varying from red (high mobility and low S^2) to blue (low mobility and high S^2). **B:** Ribbon diagram indicating the spectral density functions and chemical exchange properties for the different residues. The color-code in B is as follows: red, residues whose relaxation data could be fitted to Equation 3 (simplified Lipari & Szabo [1982] spectral density function); orange, Equation 3 plus chemical exchange (Equations 1 and 2); blue, Equation 4 (full Lipari & Szabo [1982] spectral density function); purple, Equation 4 plus chemical exchange; and green, Equation 5 (extended spectral density function). The coordinates are taken from Gronenborn et al. (1991) and have the PDB accession code number 1GB1; the model in A was made using the program O (Jones & Kjeldgaard, 1992) and that in B using the program Ribbons (Carson, 1987).

both the picosecond and slower time scales (such as those that give rise to chemical exchange line broadening) but also, and more importantly, to the packing density of the protons.

In the case of four (Leu 12, Glu 42, Asp 46, and Thr 49) of the six residues whose generalized order parameter lies below 1SD of the mean, the relaxation data could only be accounted for by Equation 5. In addition, there are three other residues whose relaxation data could only be fit using Equation 5: Thr 17, Asn 37, and Lys 50. In each case, these residues, which are represented in green in Figure 3B, are located at the ends of structural elements. The simplest physical model for the spectral density function given by Equation 5 is one in which the slow motion is represented by a jump between two states, i and j , while the fast librational motion is represented as free diffusion within two axially symmetric cones, centered about the two states i and j (Clare et al., 1990a, 1990b). The computed angle between the NH vectors in the two states ranges from 26° for

Asn 37 (located at the C-terminus of the helix) to 45° for Leu 12 (located at the C-terminus of β -strand 1), with a mean value of $35 \pm 6^\circ$ (Fig. 2I). Molecular dynamics simulations on interleukin-1 β (Chandrasekhar et al., 1992) have suggested that the slow motion involves large-amplitude jumps between conformations stabilized by hydrogen bonds, thereby permitting the NH vectors to jump between states with well-defined orientations. Examination of the structure of the IgG-binding domain indicates that the NH protons of these seven residues all participate in backbone hydrogen bonds (Gronenborn et al., 1991).

The data also provide evidence for motion on a time scale ranging from 170 ns to 2.25 ms (Powers et al., 1992) in the form of exchange line broadening (i.e., the fits to the relaxation data necessitate the use of Equations 1 and 2). These residues (indicated by orange and purple in Fig. 3B for residues that fit the spectral density functions given by Equations 3 and 4, respectively) are located primarily in the central region of β -strand 2,

most of the helix, the C-terminus of β -strand 3, and the N- and C-termini of β -strand 4. The increase in linewidth, however, is small, ranging from 0.08 to 0.34 Hz at 600 MHz, with a mean value of 0.16 ± 0.08 Hz. The largest increases in linewidth are seen for Ala 23, Thr 25, and Lys 28 in the helix (Fig. 2E). It is tempting to suggest, as in the case of interleukin-8 (Grasberger et al., 1993), that the exchange line broadening can be attributed to a very small rigid body rotational motion of the helix on top of the underlying sheet.

Concluding remarks

In this paper we have characterized the backbone dynamics of the IgG-binding domain of protein G by analysis of ^{15}N relaxation data at two spectrometer frequencies. By increasing the ratio of experimental observables to fitted parameters, this has permitted us to analyze the data with a greater degree of confidence than would have been possible at a single spectrometer frequency. It is tempting to draw certain conclusions about the internal motions of the IgG-binding domain in relation to its structure. The inner parallel strands, $\beta 1$ and $\beta 4$, of the β -sheet are essentially rigid. This is not surprising, as both of these strands are hydrogen bonded to two adjacent strands on either side of them. Also typical is the higher degree of mobility of the turns and loops relative to the secondary structure elements, arising presumably from the fact that these residues are involved in only a small number of close packing interactions. The outer strands ($\beta 2$ and $\beta 3$) of the sheet, and in particular β -strand 2, are more mobile than the inner two strands. Moreover, β -strand 2 not only has lower-order parameters than the other strands but also has a significant proportion of residues that manifest chemical exchange line broadening arising from a slower motion on the nanosecond to millisecond time scale. Likewise, most of the overlying helix also manifests chemical exchange line broadening, although on the picosecond time scale it is relatively rigid, as manifested by high values of S^2 . In this regard it is interesting to note that many of the residues that display chemical exchange are located in the helix and at the edges of the β -sheet (Fig. 3B). This suggests that the observed line broadening may be due to small fluctuating motions arising from the curling of the sheet around the helix.

Materials and methods

The 56-residue IgG-binding domain of protein G was expressed, uniformly ($>95\%$) ^{15}N -labeled, and purified as described previously (Gronenborn & Clore, 1993). The sample for NMR contained 1.4 mM protein in 90% $\text{H}_2\text{O}/10\%$ D_2O , 100 mM sodium acetate-d3 buffer, pH 4.3. All experiments were performed at both 500 and 600 MHz on Bruker AM500, AMX500, or AM600 spectrometers.

The ^{15}N relaxation data were obtained exactly as described previously (Grasberger et al., 1993). ^{15}N T_1 values were obtained using seven T delays of 14.51, 43.64, 101.90, 198.99, 393.18, 635.92, and 878.66 ms, and ^{15}N T_2 values were obtained with eight T delays of 14.31, 28.62, 57.24, 85.86, 114.48, 171.72, 228.97, and 286.21 ms. The recycle time was 1.2 s for the ^{15}N T_1 and T_2 experiments and 3 s for the NOE experiments. The decays of cross-peak intensities with time in the ^{15}N T_1 and T_2 experiments are exponential within experimental error, and the decays were fit to a single exponential by nonlin-

ear least-squares Powell minimization using the program FACSIMILE (Chance et al., 1979; Clore, 1983). The errors in the T_1 and T_2 values were obtained from conventional analysis of the variance-covariance matrix generated by the nonlinear least-squares optimization routine. The errors in the ^{15}N T_1 and T_2 values were generally $\leq 5\%$. The errors in the NOE measurements were on the order of ± 0.1 . In addition, a systematic error of no more than 20% in the absolute value of the NOE may arise from chemical exchange with water, assuming a T_1 of 2.5 s for water in an NOE experiment with a recycle delay of 3 s (Clore et al., 1990a). However, as the pH of the sample was low (pH 4.3) and as 75% of the backbone amides are involved in hydrogen bonds, this effect is likely to be minimal.

Acknowledgments

This work was supported by the AIDS Targeted Antiviral Program of the Office of the Director of the National Institutes of Health (G.M.C., A.M.G.).

References

- Achari A, Hale SP, Howard AJ, Clore GM, Gronenborn AM, Hardman KD, Whitlow M. 1992. 1.67-Å X-ray structure of the B2 immunoglobulin-binding domain of streptococcal protein G and comparison to the NMR structure of the B1 domain. *Biochemistry* 31:10449-10457.
- Boyd J, Hommel U, Campbell ID. 1990. Influence of cross-correlation between dipolar and anisotropic chemical shift relaxation mechanisms upon longitudinal relaxation rates of ^{15}N in macromolecules. *Chem Phys Lett* 175:477-482.
- Boyle NDP. 1990. *Bacterial immunoglobulin binding proteins*. San Diego: Academic Press.
- Carson M. 1987. Ribbon models of macromolecules. *J Mol Graphics* 5:103-106.
- Chance EM, Curtis AR, Jones IP, Kirby CR. 1979. FACSIMILE: A computer program for flow and chemistry simulation, and general initial value problems. *UK Atomic Energy Authority, Harwell (Rep.) AERE-R 8775*.
- Chandrasekhar I, Clore GM, Szabo A, Gronenborn AM, Brooks BR. 1992. A 500 ps molecular dynamics simulation study of interleukin-1 β in water: Correlation with nuclear magnetic resonance spectroscopy and crystallography. *J Mol Biol* 226:239-250.
- Clore GM. 1983. Computer analysis of transient kinetic data. In: Geisow MJ, Barrett M, eds. *Computing in biological science*. Amsterdam: Elsevier North-Holland. pp 313-348.
- Clore GM, Driscoll PC, Wingfield PT, Gronenborn AM. 1990a. Analysis of the backbone dynamics of interleukin-1 β using two-dimensional inverse detected heteronuclear ^{15}N - ^1H NMR spectroscopy. *Biochemistry* 29:7387-7401.
- Clore GM, Gronenborn AM. 1992. Localization of bound water in the solution structure of the immunoglobulin binding domain of streptococcal protein G. *J Mol Biol* 223:853-856.
- Clore GM, Robien MA, Gronenborn AM. 1993. Exploring the limits of precision and accuracy of protein structures determined by nuclear magnetic resonance spectroscopy. *J Mol Biol* 231:82-102.
- Clore GM, Szabo A, Bax A, Kay LE, Driscoll PC, Gronenborn AM. 1990b. Deviations from the simple two-parameter model-free approach to the interpretation of nitrogen-15 nuclear magnetic resonance of proteins. *J Am Chem Soc* 112:4989-4991.
- Fahnestock SR, Alexander P, Filpula D, Nagle J. 1990. Structure and evolution of the streptococcal genes encoding protein G. In: Boyle NDP, ed. *Bacterial immunoglobulin binding proteins, vol 1*. New York: Academic Press. pp 133-148.
- Grasberger BL, Gronenborn AM, Clore GM. 1993. Analysis of the backbone dynamics of interleukin-8 by ^{15}N relaxation measurements. *J Mol Biol* 230:364-372.
- Gronenborn AM, Clore GM. 1993a. Structural studies of immunoglobulin-binding domains of streptococcal protein G. *ImmunoMethods* 2:3-8.
- Gronenborn AM, Clore GM. 1993b. Identification of the contact surface of a streptococcal protein G domain complexed with a human Fc fragment. *J Mol Biol* 233:331-335.
- Gronenborn AM, Filpula DR, Essig NZ, Achari A, Whitlow M, Wingfield

- PT, Clore GM. 1991. A novel, highly stable fold of the immunoglobulin binding domain of streptococcal protein G. *Science* 253:657-661.
- Jones TA, Kjeldgaard M. 1992. *O—The manual version 5.8.1*. Uppsala, Sweden: University of Uppsala.
- Kay LE, Nicholson LK, Delaglio F, Bax A, Torchia DA. 1992. The effects of cross-correlation between dipolar and chemical shift anisotropy relaxation mechanisms on the measurement of T_1 and T_2 values in proteins: Pulse sequences for the removal of such effects. *J Magn Reson* 97:359-375.
- Kay LE, Torchia DA, Bax A. 1989. Backbone dynamics of proteins as studied by ^{15}N inverse detected heteronuclear NMR spectroscopy: Application to staphylococcal nuclease. *Biochemistry* 28:8972-8979.
- Kördel J, Skelton NJ, Akke M, Palmer AG, Chazin WJ. 1992. Backbone dynamics of calcium-loaded calbindin D9k studied by two-dimensional proton detected ^{15}N NMR spectroscopy. *Biochemistry* 31:4856-4866.
- Lipari G, Szabo A. 1982. Model-free approach to the interpretation of nuclear magnetic resonance relaxation in macromolecules. 1. Theory and range of validity. *J Am Chem Soc* 104:4546-4559.
- Palmer AG, Skelton NJ, Chazin WJ, Wright PE, Rance M. 1992. Suppression of cross-correlation between dipolar and anisotropic chemical shift relaxation mechanisms in the measurement of spin-spin relaxation rates. *Mol Phys* 75:699-711.
- Peng JW, Wagner J. 1992. Mapping of spectral densities of N-H bond motions in eglin c using heteronuclear relaxation experiments. *Biochemistry* 31:8571-8586.
- Powers R, Clore GM, Garrett DS, Gronenborn AM. 1993. Relationships between the precision of high resolution protein NMR structures, solution order parameters, and crystallographic B factors. *J Magn Reson Ser B* 101:325-327.
- Powers R, Clore GM, Stahl SJ, Wingfield PT, Gronenborn AM. 1992. Analysis of the backbone dynamics of the ribonuclease H domain of the human immunodeficiency virus reverse transcriptase using ^{15}N relaxation measurements. *Biochemistry* 31:9150-9157.
- Redfield C, Boyd J, Smith LJ, Smith RAG, Dobson CM. 1992. Loop mobility in a four helix-bundle protein: ^{15}N NMR relaxation measurements of interleukin-4. *Biochemistry* 31:10431-10437.
- Ringe D, Petsko GA. 1985. Mapping protein dynamics by X-ray diffraction. *Progr Biophys Mol Biol* 45:197-235.
- Schneider DM, Dellwo MJ, Wand AJ. 1992. Fast internal main-chain dynamics of human ubiquitin. *Biochemistry* 31:3645-3652.